RSC Advances

ROYAL SOCIETY OF CHEMISTRY

www.rsc.org/advances

For publication in: RSC Advances (Revised)

Occurrence of a functionally stable photoharvesting single peptide allophycocyanin *α*-subunit (16.4 kDa) in the cyanobacterium *Nostoc* sp. R76DM

Rajesh P Rastogi*[§], Ravi R Sonani[§], Avani B Patel, Datta Madamwar*

BRD School of Biosciences, Sardar Patel University, Vadtal Road, Satellite Campus, Vallabh Vidyanagar 388120, Gujarat, India.

*Corresponding author. Tel.: +91 02692 229380; fax: +91 02692 231042/236475.

E-mail addresses: raj_rastogi@rediffmail.com (R.P. Rastogi), ravi123sonani@gmail.com (R.R. Sonani), datta_madamwar@yahoo.com (D. Madamwar).

[§] Contributed equally

Abstract

The allophycocyanin (APC) is the primary photoreceptors, usually composed of *α*- and *β*-polypeptide subunits. Herein, we report the occurrence of a functionally stable single peptide APC α-subunit in the cyanobacterium *Nostoc* sp. R76DM. APC was purified successfully by ammonium sulfate fractionation. A series of biochemical characterizations like SDS-PAGE, native-PAGE, UV-visible spectroscopy, fluorescence spectroscopy and circular dichroism were performed ensuring the purity, integrity and functionality of purified APC. Matrix-assisted laser-desorption ionization time-of-flight mass spectrometry (MALDI-TOF-MS) analysis of intact PBP revealed a ~16.4 kDa protein. MS/MS spectrum of four major peptides 1051, 1431, 3209 and 2163 Da of trypsin digested purified PBP followed by amino acid sequences of these peptides shows high degree (100 %) sequence similarities with that of APC *α*-subunit (accession no. P16570, UniProtKB). The absorption as well as fluorescence spectra of single peptide APC *α*-subunit was shifted from normal absorption at 652 nm to 613 nm and fluorescence at 663 nm to 645 nm. Urea-induced denaturation based Gibbs-free energy (ΔG_D°) calculations suggested the folding and structural stability of APC *α*-subunit almost similar to that of standard APC (*αβ*) heterodimer from *Lyngbya* sp. Moreover, due to conserved structural and functional integrity, APC *α*-subunit may widely be used as a relatively low molecular weight fluorescent tag for fluorescence detection techniques.

Keywords: cyanobacteria, phycobiliprotein, allophycocyanin, stability, fluorescence, single peptide

1. Introduction

Cyanobacteria are ubiquitous in nature and are major contributors to the evolution of atmospheric oxygen. They are immense source of several high value compounds[1] in connection with the most vital life supporting biological phenomena, the photosynthesis.[2] Phycobiliproteins (PBPs) such as phycorerythrin (PE), phycocyanin (PC) and allophycocyanin (APC) are core photoharvesting pigment biomolecules crucial for photosynthesis in cyanobacteria and red algae. These biliproteins are associated with the light-harvesting complex (or antenna complex) of a photosystem called phycobilisome (PBS). Morphologically, PBS consists of a core located near the photosynthetic reaction center, most proximal to the outer surface of thylakoid membrane from which some rod-like structures are projected outwardly. The rod element of a PBS mainly contain PC (λ_{max}: ~610 and 620 nm) and/or PE (λ_{max}: ~540 and 570 nm) and linker proteins; whereas core contains the PBP APC (λ_{max}: ~600 and 680 nm). In the course of photosynthesis solar energy traverses unidirectional down the rods of the PBS where light energy can be shifted from PE via PC to the APC in the core, and subsequently, some other core biliproteins permit this absorbed light energy to chlorophyll within the thylakoid membrane. The unique spectral properties of a particular PBP depends on the presence of some chromophores such as phycocyanobilin, phycoerythrobilin, phycourobilin and phycoviolobilin attach covalently to the PBP-apoproteins.[3]

PBPs are considered as major metabolic product of cyanobacteria as almost 20 % of the total dry weight of cyanobacteria is composed of PBPs.[4] The unique color, non-toxic protein nature, strong antioxidant capacity and an exclusive absorption and fluorescence emission property of PBPs makes them ecologically as well as economically very important. In recent decades, PBPs are extensively used in food, cosmetic and pharmaceutical industries. Furthermore, some imperative properties of PBPs like hepato-protective[5], anti-oxidants[6,7],

anti-aging[8,9] and anti-inflammatory activity[10] make them highly promising macromolecules for therapeutic, diagnostic and pharmacological applications.

Structurally, most biliproteins generally exists in heterodimeric forms composed of alpha (α) and beta (β) subunits.[11] The amino acid sequence of APC from *Mastigocladus laminosus* revealed the occurrence of 160 and 161 amino acid residues for α- and β- subunits, respectively, exhibiting a high affinity for one another with 37 % homology.[12] Moreover, self-assembly of all PBP is initiated by the docking of α- and β- subunits that are only impartially homologous at amino acid sequence level (25 % – 40 %) but are highly homologous at three-dimensional structural level.[13,14] Native APC is a trimeric protein, consisting of three ($\alpha\beta$) monomers.[15] Each α- and β- subunits of APC contain a single covalently attached chromophore phycocyanobilin (PCB) that assist to construct the functional α-β dimer, the building block of PBP assembly.[16,17] It has been reported that the stability and functionality of APC $(\alpha\beta)_3$ trimer are mainly due to polar enhanced hydrophobicity of the PCB binding pocket.[18]

Some reports have described the alternative forms of PBP from cyanobacteria and red algae. Thomas and Passaquet (1999) have reported a PE composed of only β-subunit from unicellular red algae.[19] A degenerated form of PE made up of only β-subunit has been reported from a marine cyanobacterium *Prochlorococcus* sp. growing under intense light condition.[20,21] In the previous study, our group have also reported some fragmented-PE, composed of only truncated α-subunit from the marine cyanobacterium *Phormidium* sp.[22,23] and *Lyngbya* sp. A09DM.[24] Contrary to PC and PE, a few works have been conducted on general physiology and biochemistry of APC from cyanobacteria or red algae. In the study presented here, we have reported the occurrence of a functionally stable APC composed of a single peptide α-subunit from the fresh water cyanobacterium *Nostoc* sp. R76DM. As best of

our knowledge there are no reports on the occurrence and *in vivo* biosynthesis of a single peptide APC from any cyanobacterial species/strains studied so far.

2. Material and methods

2.1. Cyanobacterium and growth conditions

The cyanobacterium *Nostoc* sp. R76DM was routinely grown under axenic conditions in a BG11 liquid culture medium[25] in a culture room at 27 ± 2°C with 12:12 h light:dark cycles and illumination of 12 Wm^{-2} with cool white fluorescent lamps. The cyanobacterium was identified on the basis of 16S-rRNA gene sequence homology (accession number KJ994254).

2.2. Extraction and purification of allophycocyanin (APC)

Grown cell mass was subjected to ultra-sonication using metal-probe to homogenize the cyanobacterial cell aggregates (VC505, Vibra Cell, Sonics and Material Inc., USA). Homogenized cell mass was freezed (at -25℃) and thawed (at 4℃) to achieve cell lysis and maximum extraction of intracellular stuff with phycobiliproteins (PBPs). The cell extract obtained in this way was subjected to ammonium sulfate precipitation to separate the PBP from other impurities as described earlier.[26] Separated PBPs were further passed through DEAE-cellulose anionic exchange column to yield pure APC. The fractions containing pure APC were concentrated by ultra-filtration using a Macrosep® (10kDa MWCO centrifugal device, Pall Corporation). Purification was carried out under dark condition at 4°C unless specified. The purity of APC was recorded as 'purity ratio' calculated by formulas A_{613}/A_{280}, where A_x stands for the absorbance at X nm wavelength.

2.3. Characterization of APC

2.3.1. Gel electrophoresis analysis

Analysis of purified APCs (5 µg of each) was resolved on native- and SDS-PAGE as described earlier.[27] Proteins on resolved gels were visualized by silver and zinc-acetate staining as described earlier.[28]

2.3.2. Spectroscopic analysis

Spectroscopic analysis of purified APCs (0.4 mg ml^{-1}) was performed using a UV–Vis spectrophotometer (Specord 210, AnalytikJena AG, Jena, Germany). The data were recorded over 250–750 nm wavelength range using cuvette of 1 cm path length. The purity of standard dimeric APC (isolated from *Lyngbya* sp.) as well as single peptide APC (form *Nostoc* sp.) was verified as 'purity ratio' calculated by the formula A_{653}/A_{280} and A_{613}/A_{280}, respectively.

The fluorescence emission of APC was measured at room temperature by fluorescence spectrophotometer (F-7000, Hitachi High Technologies Corp.) to verify their functionality upon excitation at 589 nm. The raw data were transferred to a microcomputer and both absorption and emission peaks were analyzed with the respective software provided by the manufacturer.

2.3.3. Circular dichroism (CD) measurement

The far-UV CD measurement of APC was performed using Jasco spectropolarimeter (J-810). The instrument was equipped with peltier type of temperature controller (PTC-348WI). CD spectra of APC samples were collected in the wavelength range of 250–200 with a response time of 1 sec and a scan speed of 100 nm min^{-1}. All measurements were carried out at 25 ± 0.1 °C. Molar elipticity at 222 nm ($[\theta]_{222}$) was used as probe to investigate the secondary structure of protein.

2.3.4. High performance liquid chromatography (HPLC)

HPLC was performed in non-denaturing and denaturing conditions to determine the molecular weights of intact and monomerized Nostoc APC. Bio-Sil SEC 125-5 gel filtration column was used with ultra-fast liquid chromatography (UFLC, Shimazdu) systems. The results were interpreted with HP Chemstation software.

Operating parameters: Mobile phase - 50 mM potassium phosphate buffer (pH 8.0), column back pressure – 55 kg cm-2, column temperature: 25oC, protein detection: PDA detector (at 280 nm).

2.4. Gel elution, trypsin digestion of intact APC

The purified APC α-subunit (0.06 mg) was electrophoresed on sodium dodecyl sulfate (SDS)-polyacrylamide (15 %) gels. The desired protein on the resolving gel was stained with Coomassie Brilliant Blue G250 dye and the portion of an envisioned stained band of APC was cut carefully using a sterile razor blade and subjected to in-gel trypsin digestion by Trypsin-Gold (Promega Corp., Madison, WI, USA) according to manufacturer's protocol. Digested protein sample was dried and re-solubilized in trifluoroacetic acid (TFA; 0.1 %). Finally, the solution was purified by passing through Millipore®ZipTips (Sigma–Aldorich, USA) with TA buffer (0.1 % TFA + acetonitrile; 1:1 *v*/*v*) as described earlier.[29]

2.4.1. MALDI-TOF-MS analysis

To evaluate the molecular weight of pure intact peptide, matrix-assisted laser desorption/ionization time-of-flight mass spectrometry (MALDI-TOF-MS) was performed using a AB Sciex TOF/TOF™ 2046 system as described by Benedetti et al. (2006)[30] with slight modification. Briefly, 2 µl of the purified APC (15-20 pmol μl^{-1}) dissolved in potassium phosphate buffer (20 mM, pH 7.0) was mixed with sinapinic acid matrix (in TFA).

The sample was eluted directly onto the MALDI target, allowed to dry at room temperature and analyzed by the MASSLYNX program.

2.4.2. MS/MS analysis

Tryptic digested proteins were mixed with α-cyano-4-hydroxycinnamic acid (5 mg ml^{-1}) TA buffer and small quantity of the solution (2 µl) was allowed to dry on MALDI plate before MS analysis. Peptide mass fingerprinting was obtained in the positive ion mode by the MALDI-TOF/TOF mass spectrometer (ULTRAFLEXIII, Bruker Daltonics, USA). Mass spectra of selected peptides were recorded over 4000 *m/z* using the ionization conditions as described earlier.[29,30]

2.5. Bioinformatics analysis

Peptide mass fingerprints were analyzed by Flex analysis software to extract peak list. Selected peptide identification was performed by searching in a non-redundant protein sequence database (NCBInr) using Mascot program (http://www.matrixscience.com). Mascot search was performed using the parameters such as significance threshold: $p< 0.05$, enzyme: trypsin, fixed modifications: carbamidomethylation (C), variable modifications: oxidation (M), peptide mass tolerance: ± 80 ppm, maximum missed cleavages: 2 and fragment mass tolerance: ±1 Da.

The secondary and tertiary structures of APC α-chain (accession no. P16570, UniProtKB) was predicted using RaptorX server (http://raptorx.uchicago.edu/).[31] Image of tertiary structure was generated using PyMOL software (http://www.pymol.org/).[32]

2.6. *In vivo* and *in vitro* stability experiments

198 To observe the in vivo stability and nullifying the hypothesis of truncation, the PBPs were
199 extracted and purified from 10, 20, 30, 40, 50 and 60 days grown cyanobacterium. The
200 purified PBPs from log-phase culture were stored at 4^{o}C for 180 days to see the possibility of
201 truncation during long term storage period. All the biliproteins isolated from different days
202 grown cultures as well as long term (upto 20 to 180 days) stored samples were analyzed by
203 SDS-PAGE for their *in vivo* and *in vitro* stability, respectively.
204 Furthermore, *in vitro* stability of PBPs was also investigated under three different physico-
205 chemical stressors such as temperature, pH and strong oxidizing agent. Thermal stability of
206 purified APC α-subunit was investigated by exposing the APC solutions to temperatures 20,
207 40, 60 and 80 ± 2 ^{o}C for 60 min in an incubator (Innova 42, New Brunswick Scientific Co.,
208 New Jersey). To observe the effects of pH and oxidizing agent (H_2O_2) the freeze-dried
209 samples (1 mg) of APC α-subunit were re-dissolved in 20 mM potassium phosphate buffers
210 (100 μL) of different pHs (i.e., 2, 4, 6, 7, 8, 10 and 12) and percentage of H_2O_2 (i.e., 0.2, 0.4,
211 0.8 and 1.0 %.), respectively and incubated for an hour under dark condition.
212

213 **2.7. Chemical denaturation and renaturation study**

214 Chemical-induced denaturation of purified APC was studied using an organic compound urea
215 (CH_4N_2O) as described earlier (Sonani et al., 2015). In brief, increasing amount of urea was
216 mixed with protein and denaturation was allowed for 45 min at 25 °C. Whereas, renaturation
217 was performed by diluting the reaction mixture containing 9.0 M Urea. Absorption spectra of
218 denatured/renatured APC (0.2–0.4 mg ml^{-1}) were measured as described in section 2.3.2 with
219 scan range of 200-300 nm. All spectral measurements were done in triplicates.
220

221 **2.7.1. Data analysis**

The plot of change in molar extinction coefficient, $\Delta\varepsilon$ vs. [Urea] was generated using UV-visible results. This plot was used for the calculation of $\Delta G_D°$ (Gibbs free energy change for denaturation of protein), *m* (slope of the plot of $\Delta G_D°$, the Gibbs free energy change vs. [urea], i.e., $\partial\Delta GD/\partial$ [urea]) and *Cm* (midpoint of denaturation curve, i.e., [urea] at which $\Delta G_D° = 0$). The linear relationship between ΔG_D and [Urea] was assumed and expressed by

$y = y_N + y_D \times Exp [- (\Delta G_D°- m [Denaturant])/RT]/(1+(Exp [- (\Delta G_D°- m [Denaturant])/RT])$ ---- (Equation-1).

Where, y_N and y_D are the spectral properties of the native (N) and denatured (D) state of protein, R is gas constant and T is the temperature in Kelvin (K).

3. Results and discussion

3.1. Extraction, fractionation and purification of PBP

The sequential freeze-thaw actions of cyanobacterial cell mass caused the release of intracellular contents with the photo-harvesting PBP pigments. All the biliproteins released out of the cells were purified by different concentrations of ammonium sulfate precipitation followed by chromatographic techniques. The purity ratios of APC from *Nostoc* sp. established after different fractionation was found up to 3.12 (Table 1). The APC obtained from *Lyngbya* sp.[7] was used as a standard (hereafter S-APC) against the APC from *Nostoc* sp (hereafter N-APC).

Furthermore, the purity of APC was affirmed by manifestation of SDS-PAGE. Contrary to S-APC, only one band of N-APC corresponding to a smaller subunit of PBP was observed without detectable contaminations in the cyanobacterium *Nostoc* sp. (Fig. 1A). UV-Visible spectrum of N-APC (λ_{max}: 613 nm) as well as S-APC (λ_{max}: 652 nm) showed the high purity of APCs as the peak of N-APC and S-APC was highly prominent over the peak at 280 nm (Fig. 1B). Ammonium sulfate precipitation and aqueous two phase separation (ATPS) are

well established tools for PBPs separation and purification.[4,33] Several methods have been described to extract and purify the specific biliproteins from different cyanobacteria[34]; however, our group has recently reported an efficient technique for concurrent purification of all three major PBPs from *Lyngbya* sp. A09DM.[7] Contrary to phycoerythrin (PE) and phycocyanin (PC), the purification of allophycocyanin (APC) is very arduous due to its availability in very low quantity and/or lower resolution to discriminate between their surface hydrophobic properties; however, in the present study, a high concentration (59.45 % of crude extract) of a single peptide APC was purified from the cyanobacterium *Nostoc* sp. R76DM.

3.2. Characterization of APC

The purified APC from *Nostoc* sp. R76DM was chemically as well as structurally and functionally characterized using a series of biochemical characterizations like SDS-PAGE, native-PAGE, UV-visible spectroscopy, fluorescence spectroscopy, circular dichroism and MALDI-TOF-MS.

Silver stained SDS-PAGE (Fig. 1A) of purified N-APC along with the high range protein markers revealed a single band with molecular weight of about ~16.4-17.5 kDa. Zinc acetate stained SDS-PAGE of purified N-APC also showed a single distinct fluorescent bands under UV light, and this band co-migrated with the ~16.4-17.5 kDa silver stained band, indicating the presence of chromophore/s linked to the single peptide APC from *Nostoc* sp. (Fig. 1A). MALDI-TOF-MS spectrum of intact N-APC also showed a significant peak of a major component of *m/z* 16.4 kDa (Fig. 2). Moreover, results obtained by electrophoresis (Fig. 1A) and mass spectrometry (Fig. 2) confirmed the existence of a single peptide PBP without the existence of any contaminating proteins. Moreover, the appearance of a similar peak (with ~17.50 RT) in HPLC- chromatograms of *Nostoc* APC under non-denaturing and

denaturing conditions indicated the existence of APC in non-oligomeric form (Sup. Figure S1).

The resulted molecular mass (i.e., 16.4 kDa) is more or less close to those of other single peptide PBPs isolated from different cyanobacteria. Recently, Sonani et al. (2015)[24] have characterized a single peptide phycoerythrin (15.45 kDa) from *Lyngbya* sp. A09DM. Parmar et al. (2011)[23] have characterized a 14 kDa functional α-subunit PE from marine cyanobacterium *Phormidium* sp. A27DM. Moreover, all the PBPs characterized as single peptide α-and/or β-subuint from different cyanobacteria were the results of truncation by means of different abiotic factors. [22,23] However, herein we report the biosynthesis of a single peptide α-subunit APC from the cyanobacterium *Nostoc* sp. growing under natural conditions without any external abiotic influence.

3.2.1. Characterization of APC subunit composition

Pure fractions of single peptide PBP (from *Nostoc* sp.) as determined by their electrophoretic and mass composition were carried out for a matrix-assisted laser desorption ionization (MALDI) peptide mass fingerprint (PMF) to identify the subunit composition of single peptide APC. The mass spectrum showed several protonated ions $[M+H]^+$ of the peptide fragments as shown in Figure 3. Amino acid sequences of five major peptides i.e., 1051 (Fig. 3A), 1431 (Fig. 3B), 936 (Fig. 3C), 2291 (Fig. 3D) and 2163 Da (Fig. 3E) deduced from MS/MS analysis of trypsin digested single peptide APC was hit in NCBInr protein sequencing database by Mascot peptide fingerprint search engine with full APC alpha chain of *Microchaete diplosiphon* with top protein scores > 92 and $P < 0.05$. Moreover, Mascot similarity search has revealed 100 % sequence similarities of these peptides with APC α-subunit (accession no. P16570) (Fig. 3F). Furthermore, the results obtained from MALDI-

296 TOF and PMF analysis clearly identify the purified PBP as single peptide APC α-subunit
297 (Sup. Figure S2).

298 Recently, some studies have been conducted to synthesize the stable single peptide *β*-
299 subunit in the metabolically engineered *Escherichia coli* cells.[35,36] The biosynthesis of a
300 recombinant APC *β*-subunit from a cyanobacterium was successfully reconstituted in *E. coli*
301 which spectroscopic properties were similar to native APC.[36] Moreover, the present study
302 would be helpful in understanding the uniqueness of photosynthetic machinery of
303 cyanobacteria and promising use of single peptide APC as fluorescent tag as a substitute for
304 native APC.

305 The APC alpha chain structure was predicted using sequence form *Microchaete diplosiphon*.
306 The three-state secondary structure of *Microchaete* APC was predicted and represented by
307 helix, beta-sheet and loop with 74 %, 3 % and 21 % of sequences, respectively (Fig 4).
308 Predicted 3D structure showed eight alpha helices (modelled residues-161) (Fig 4). The p-
309 value of predicted structure was 1.13e-05, which indicated good quality of structure. MS/MS
310 derived four different peptides (i.e., 1051 Da, 1431 Da, 3209 Da, and 2163 Da) having
311 sequence similarities with that of APC α-subunit (accession no. P16570, UniProtKB) were
312 shown in red (A), blue (B), magentas (C) and orange (D) colors, respectively (Fig 4).

313

314 **3.2.2. Functional characterization of APC**

315 The functionality of the single peptide APC pigment was further analyzed with regard to its
316 spectral characteristics using far-UV CD, absorption and emission. The data clearly showed
317 the functionality of APC α-subunit bearing bilin chromophores (as revealed by Zn-acetate
318 staining) with an absorption maximum at 613 nm and fluorescence emission at 645 nm (Fig.
319 5A). However, the absorption as well as fluorescence spectra of single peptide APC *α*-subunit
320 was shifted from normal absorption and fluorescence emission of a heterodimeric (*αβ*)

standard APC (from *Lyngbya* sp.) at 652 nm and 663 nm, respectively (Fig. 5B). The far-UV CD spectrum of the native APC α-subunit exhibited double minima at 208 and 222 nm (Fig. 6), indicating its preserved substantial secondary structure. These values revealing the functionality of purified APC α-subunit are in consistent with those of previous reports.[37]

3.3. Folding and stability dynamics of single peptide α-subunit APC

In vitro denaturation and renaturation capability of α-subunit APC was studied using urea (CH_4N_2O) as a denaturing agent. Folding/unfolding of N-APC and S-APC was performed by recording the changes in their UV-Visible absorption maxima at 613 (Fig. 7A) and 652 nm (Fig. 7B), respectively. Absorption spectra of both biliproteins were measured in the range of 250-750 nm to check the difference in their structural stability as the function of variable urea concentrations. The absorbance of both α-subunits APC (Fig. 7A) as well as standard heterodimeric APC (Fig. 7B) was found to decrease successively with the increase in urea concentration, which are in agreement with those determined previously on other PBP.[24,38] It has been determined that the unique absorption characteristics of APC is due to the presence or interaction between a chromophore PCB and respective apoprotein.[16,17] Moreover, decrease in specific absorbance of a biliprotein might be due to the loss/alteration of chromophore-apoprotein interaction or specific level of protein folding.[39,40,41] A significant loss of APC absorbance was observed up to 4 M urea; however, no significant difference in absorbance properties was observed above 5-6 M urea, probably due to the decrease in the rigidity of chromophores configurations in the native protein caused by balanced hydrophilic/hydrophobic network distraction.[42] Figure 7C and 7D shows the denaturation curves of a single peptide APC α-subunit and standard heterodimeric APC plotted against difference in molar absorption coefficients (ε) at 613 nm ($\Delta\varepsilon_{613}$) and 652 nm ($\Delta\varepsilon_{652}$), respectively, as the function of presence or absence of urea. The trend of denaturation-

renaturation phenomena for single peptide APC α-subunit was similar to those of standard heterodimeric APC, suggesting the basic structural integrity of novel APC α-subunit from *Nostoc* sp. The plots of $\Delta\varepsilon_{613}$ and $\Delta\varepsilon_{652}$ as the function of urea were analyzed for ΔG_D^o, m, and C_m values for each APC protein in relation to equation-1, and depicted in Table 2. The data obtained from denaturation and/or renaturation process distinctly revealed that denaturation of APC is a two-state reversible process as also described in our previous study using the other PBPs.[24,38] It has been stated that two-state mechanisms of denaturation-renaturation of a particular protein depends on the coincidence of the normalized sigmoidal curves of several physical properties induced by certain denaturing agents such as urea.[38] However, non-coincidence of sigmoidal curves of different physical properties of a protein may also regulate two-state protein folding/unfolding characteristics.[43-44] Furthermore, two-state folding/unfolding behavior of a protein as the function of urea can be monitored by observed values of ΔG_D^o.[45] In the present study, the values of ΔG_D^o (protein stability) of single peptide APC α-subunit (3.98 ± 0.18 kcal mol^{-1} M^{-1}) from *Nostoc* sp. and standard heterodimeric APC (4.12 ± 0.21 kcal mol^{-1} M^{-1}) from *Lyngbya* sp. was almost similar (Table 2), indicating the conserved geometry of APC α-subunit.

3.3.1. Thermal and chemical stability of α-subunit APC

Stability of a protein against different physico-chemical factors is utmost requirement for their use in food, pharmaceuticals, cosmeceuticals and other biomedical research. We have inspected the thermal and chemical stability of α-subunit APC under different temperatures and pHs and oxidizing agent.

Figure 8A shows the UV-Visible absorption spectrum of purified APC α-subunit before and after 1 h of heat exposure. The single peptide APC α-subunit showed considerably good stability towards temperature up to 40 °C; however, degradation rate increased rapidly

371 over 60 °C (Fig. 8A). Moreover, PBPs isolated from different taxonomic groups differ in
372 their stability under different physicochemical factors including thermostability.[46-51] Similar
373 to APC α-subunit, loss of UV-visible spectral properties of heterodimeric form of APC
374 isolated from *Lyngbya* was also observed at 60-80 °C.[50] It has been found that the functional
375 property of APC is also lost at high temperature.[50] It has been suggested that the changes in
376 thermal stability of a PBP might be due to a number of sequence-dependent structural
377 changes.[52]

378 The stability of purified APC α-subunit was also investigated in a wide range of pHs.
379 Figure 8B shows the effects of different pHs on its UV-visible spectral properties. APC α-
380 subunit showed functional stability in the pH range 4.0-7.0, respectively; however, relatively
381 low stability was observed at pH 8.0 (Fig. 8B). The residual fraction of APC was severely
382 decreased under a range of acidic (pH 2.0) and alkaline (pH 10.0-12.0) conditions (Fig. 8B).
383 The PBP (B-PE) obtained from the red algae *Porphyridium cruentum* showed stronger
384 functional stability in the pH range 4.0-10.0.[49] Recently, Rastogi et al. (2015a) have observed
385 the structural and functional stability of PBPs under different physico-chemical stressors.[50]
386 The percentage decrease in dimeric APC concentration after 1 h storage at pH 2.0, 4.0, 10.0
387 and 12.0 was 56.8 ± 3.1, 48.58 ± 2.8, 72.47 ± 1.6 and 87.98 ± 1.9, respectively. Moreover,
388 both single peptide and/or dimeric APC may differ in their sensitivity towards different pH
389 conditions.

390 The incubation of the purified APC α-subunit with the oxidizing agent H_2O_2 led to a
391 successive decrease in their absorption (Fig. 8C) accompanied with disappearance of their
392 respective color (data not shown) with the increase in H_2O_2 concentration. Moreover,
393 contrary to high temperature and pHs, the spectral properties of APC was relatively
394 maintained under oxidative stress, indicating the potential of PBP as free radical scavengers.
395

3.3.2. *In vivo* and *In vitro* stability of α-subunit APC

Both *in vivo* and *in vitro* stability of purified single peptide α-subunit APC were performed. There was no additional reduction in peptide size or intensity was observed upon 180 days storage (Fig. 9A). To clarify the possibility of *in vivo* truncation in the culture growing for long term, we isolated and purified the biliproteins from the *Nostoc* cultures growing at different time intervals. Figure 9B showed the existence of similar biliproteins isolated from 10 to 60 days grown cyanobacterium cultures, indicating the *in vivo* stability of single peptide α-subunit APC. The results obtained from SDS-PAGE analysis of purified PBP (Fig. 9) directly support the synthesis of single peptide α-subunit APC and discarding or nullifying the possibilities of *in vivo* or *in vitro* PBP truncation process in the cyanobacterium *Nostoc* sp. R76DM during long-term culture storage or *in vitro* storage of purified PBP at 4°C. Moreover, the occurrence of single peptide PBPs have also been reported as a result of *in vivo* or *in vitro* truncation of PBPs in the cyanobacterium *Phormidium tenue*[22] and *Lyngbya sp.* A09DM[24], respectively.

4. Conclusions

Very few works have been reported regarding the occurrence of APC particularly on occurrence of a single peptide APC subunit. We have purified and characterize the occurrence of a single peptide APC α-subunit (16.4 kDa) in the cyanobacterium *Nostoc* sp. R76DM. Urea-induced denaturation and Gibbs-free energy (ΔG_D°) calculations suggested the folding and structural stability of APC *α*-subunit almost similar to that of standard APC (*αβ*) heterodimer from *Lyngbya* sp. The PBP APC *α*-subunit showed both *in vivo* and *in vitro* stability against long-term culture storage or storage of purified PBP at 4 °C, respectively. The occurrence of APC composed of a single subunit may reveal some changing aspects of photosynthesis in photoautotrophs. Moreover, due to conserved structural and functional

integrity, APC α-subunit may be used as a low molecular weight fluorescent tag as a constituents of relatively higher molecular weight native APC in fluorescence detection techniques for different diagnostic purposes.

Acknowledgements

Rajesh P. Rastogi is thankful to the University Grant Commission (UGC), New Delhi, India for Dr. D.S. Kothari Postdoctoral Research Grant. Ravi R. Sonani thanks the Department of Science and Technology (DST), New Delhi, India for financial help in the form of the INSPIRE (IF120712) fellowship.

References

1. R. P. Rastogi and R. P. Sinha, *Biotechnol. Adv.*, 2009, 27, 521-539.
2. N. K. Singh, R. R. Sonani, R. P. Rastogi and D. Madamwar, *EXCLI J.*, 2015, 14, 268-289.
3. K. E. Wilk, S. J. Harrop, L. Jankova, D. Edler, G. Keenan, F. Sharples, *Proc. Natl. Acad. Sci. USA*, 1999, 96, 8901-8906.
4. B. Soni, U. Trivedi and D. Madamwar, *Bioresour. Technol*. 2008, 99, 188-194.
5. D. Remirez, V. Fernandez and G. Tapia, *Inflamm. Res.*, 2002, 51, 351-356.
6. C. Romay and R. Gonzalez, *J. Pharm. Pharmacol.*, 2000, 52, 367-368.
7. R. R. Sonani, N. K. Singh, J. Kumar, D. Thakar and D. Madamwar, *Process Biochem.*, 2014, 49, 1757-1766.
8. R. R. Sonani, N. K. Singh, A. Awasthi, B. Prasad, J. Kumar and D. Madamwar, *AGE*, 2014, 36, 9717.
9. R. R. Sonani, R. P. Rastogi, D. Madamwar D, *Biochem. Anal. Biochem.*, 2015, DOI: 10.4172/2161-1009.1000172
10. M. A. Qureshi, J. D. Garlich and M. T. Kidd, *Immunopharmacol. Immuno-toxicol.* 1996, 18, 465-476.
11. R. R. Sonani, M. Sharma, G. D. Gupta, V. Kumar and D. Madamwar, *Acta Cryst. F*, 2015, 71, doi:10.1107/S2053230X15010134.
12. W. Sidler, J. Gysi, E. Isker and H. Zuber, Hoppe-Seyler´ s Zeitschrift für physiologische Chemie., 1981, 362, 611-628.
13. L. K. Anderson, and C. M. Toole, *Mol. Microbiol.*, 1998, 30, 467–474.
14. N. Adir, K. Dines, M. Klartag, A. McGregor and M. Melamed-Frank, in J. M. Shively (Eds.), Microbiology Monographs: Inclusions in Prokaryotes, Springer, Berlin, Germany, 2006, 2, 47–77.

15. R. MacColl, L. E. Eisele, and A. Menikh, *Biopolymers*, 2003, 72, 352-365.

16. J. Q. Zhao and L. J. Jiang, *Sci. China Ser. B*, 1998, 41, 520-524.

17. J. M. Zhang, Y. J. Shiu, M. Hayashi, K. K. Liang, C. H. Chang, V. Gulbinas, C. M. Yang, T. S. Yang, H. Z. Wang, Y.-T. Chen and S. H. Lin, *J. Phys. Chem. A*, 2001, 105, 8878-8891.

18. A. McGregor, M. Klartag, L. David and N. Adir. *J. Mol. Biol.*, 2008, 384, 406–421.

19. J. C. Thomas and C. Passaquet, *J. Biol. Chem.*, 1999, 274, 4, 2472-2482.

20. C. Steglich, N. Frankenberg-Dinkel, Si. Penno and W. R. Hess, *Env. Microbiol.*, 2005, 7, 1611-1618.

21. J. Wiethaus, A. W. U. Busch, T. Dammeyer and N. Frankenberg-Dinkel, Eur. J. Cell Biol., 2010, 89, 1005-1010.

22. B. R. Soni, M. I. Hasan, A. Parmar, A. S. Ethayathulla, R. P. Kumar , N. K. Singh, M. Sinha, P. Kaur, S. Yadav, S. Sharma, D. Madamwar and T. P. Singh., *J. Str. Biol.* 2010, 171, 247–255.

23. A. Parmar, N. K. Singh, A. Kaushal and D. Madamwar. *Process Biochem.*, 2011, 46, 1793-1799.

24. R. R. Sonani, R. P. Rastogi, M. Joshi and D. Madamwar, *Int. J. Biol. Macromol.*, 2015, 74, 29-35.

25. R. Rippka, J. Deruelles, J. B. Waterbury, M. Herdman and R. Y. Stanier, *J. Gen. Microbiol.*, 1979, 111, 1–61.

26. R. R. Sonani, G. D. Gupta, D. Madamwar and V. Kumar. *PLoS ONE*, 2015, 10, e0124580.

27. N. K. Singh, A. Parmar, R. R. Sonani and D. Madamwar, *Process Biochem.*, 2012, 47, 2472-2479.

28. D. Garfin, in: M.P. Deutscher, J.N. Abelson, M.I. Simon (Eds.), Guide to Protein Purification, Academic Press, California, 1990, 425-441.
29. B.J. Savary, P. Vasu, A. Nunez and R. G. Cameron, *J. Agric. Food Chem.* 2010, 58, 12462–12468.
30. S. Benedetti, S. Rinalducci, F. Benvenuti, S. Francogli, S. Pagliarani, L. Giorgi, M. Micheloni, G. M. D'Amici, L. Zolla and F. Canestrari, *J. Chromatogr. B*. 2006, 833, 12-18.
31. M. Källberg, H. Wang, S. Wang, J. Peng, Z. Wang, H. Lu and J. Xu, *Nature Prot.*, 2012, 7, 1511-1522.
32. L. Grell, C. Parkin, L. Slatest and P. A. Craig, Biochem. *Mol. Biol. Educ.*, 2006, 34, 402-407.
33. B. Soni, B. Kalavadia, U. Trivedi and D. Madamwar, *Process Biochem*., 2006, 41, 2017-2023.
34. S. K. Mishra, A. Shrivastav and S. Mishra, *Protein Expres. Purif.*, 2011, 80, 234-238.
35. B. Ge, H. Sun, Y. Feng, J. Yang and S. Qin, *J. Biosci. Bioeng.*, 2009, 107, 246-249.
36. H. Chen, H. Lin, F. Li, P. Jiang and S. Qin, *J. Biosci. Bioeng.*, 2013, 115, 485-489.
37. I. C. Hu, T. R. Lee, H. F. Lin, C. C. Chiueh, and P. C. Lyu. *Biochemistry*, 2006, 45, 7092-7099.
38. K. Anwer, R. Sonani, D. Madamwar, P. Singh, F. Khan, K. Bisetty, F. Ahmad and M. I. Hassan, *J. Biomol. Str. Dyn.*, 2015, 33, 121-133.
39. D. M. Arciero, D. A. Bryant and A. N. Glazer, *J. Biol. Chem.*, 1988, 263, 18343-18349.
40. K. Brejc, R. Ficner, R. Huber and S. Steinbacher, *J. Mol. Biol.*, 1995, 249, 424-440.
41. J. Martinez-Oyanedel, C. Contreras-Martel, C. Bruna and M. Bunster, *Biol. Res.*, 2004, 37, 733-745.

42. Y. Ma, J. Xie, C. Zhang and J. Zhao, *Biochem. Biophys. Res. Com.* 2007, 352, 787-793.

43. H. Rahaman, M. K. A. Khan, M. I. Hassan, A. Islam, and F. Ahmad, *J. Chem. Thermodyn.*, 2013, 58, 351–358.

44. K. A. Dill and D. Shortle, *Ann. Rev. Biochem.*, 1991, 60, 795–825.

45. D.W. Bolen and M. Yang, *Biochemistry*, 2000, 39, 15208-15216.

46. C. Pumas, P. Vacharapiyasophon, Y. Peerapornpisal, P. Leelapornpisid, W. Boonchum, M. Ishii and C. Khanongnuch, *Phycol. Res.*, 2011, 59, 166-174.

47. R. Chaiklahan, N. Chirasuwan and B. Bunnag, *Process Biochem.*, 2012, 47, 659-664.

48. M. Munier, S. Jubeau, A. Wijaya, M. Morançais, J. Dumay, L. Marchal, P. Jaouen, and J. Fleurence, *Food Chem.*, 2014, 150, 400-407.

49. E. González-Ramírez, M. Andújar-Sánchez, E. Ortiz-Salmerón, J. Bacarizo, C. Cuadri, T. Mazzuca-Sobczuk, M. J. Ibáñez, A. Cámara-Artigas and S. Martínez-Rodríguez, *Food Biophys.*, 2014, 9, 184-192.

50. R. P. Rastogi, R. R. Sonani and D. Madamwar, *Bioresour. Technol.*, 2015, 190, 219-226.

51. R. P. Rastogi, R. R. Sonani and D. Madamwar, *Photochem. Photobiol.*, 2015, 91, 837-844.

52. N. Adir, Y. Dobrovetsky, N. Lerner, *J. Mol. Biol.*, 2001, 313, 71–81.

545 **Table 1**: Allophycocyanin content, purity and yield at each stage of purification.

Organisms	Purification	Total protein content (mg)	APC content (mg)	Purity ratio A_{max}/A_{280}	Yield (%)
***Nostoc* APC**	**Crude**	40.18	5.18	0.29	100.00
	Purified APC	3.15	3.08	3.12	59.45
***Lyngbya* APC**	**Crude**	54.16	7.12	0.23	100.00
	Purified APC	5.38	5.17	3.09	72.61

546

547

548 **Table 2**: Denaturation kinetics of allophycocyanin from *Nostoc* and *Lyngbya* sp.

Protein	ΔG_D° (kcal mol^{-1})	M (kcal mol^{-1} M^{-1})	C_m (M)
Nostoc APC	3.98 ± 0.18	2.23 ± 0.12	1.78 ± 0.11
Lyngbya APC	4.12 ± 0.21	2.17 ± 0.09	1.89 ± 0.09

549

Figure legends

Fig. 1. (A) Silver (left panel) and zinc acetate (right panel) stained 15 % SDS-PAGE of protein molecular mass standard (Marker), APC from *Lyngbya* sp. (AP-L) and *Nostoc* sp. R76DM (AP-N). (B) UV-visible absorption spectra of purified APC from *Nostoc* sp. (a) and *Lyngbya* sp. (b) with absorption maximum at 613 nm and 652 nm, respectively.

Fig. 2. Matrix-assisted laser-desorption ionization time-of-flight mass spectrometry (MALDI-TOF-MS) spectrum of intact APC from *Nostoc* sp. R76DM.

Fig. 3. MS/MS spectra of four major peptides 1051 (A) and 11431 Da (B), 936 (C), 2291 (D) and 2163 (E) of trypsin digested APC. (E) Deduced amino acid sequences of these peptides shows 100 % sequence similarities with that of APC α-subunit (accession no. P16570, UniProtKB).

Fig. 4. A predicted secondary structure of allophycocyanin alpha chain (with helix, beta strands and coil) of *Microchaete diplosiphon* and amino acid sequence similarities of four major peptides 1051 (A) and 11431 Da (B), 3209 (C) and 2163 (D) of trypsin digested single peptide APC α-subunit from *Nostoc* sp.

Fig. 5. Absorption and fluorescence emission spectra of APC α-subunit from *Nostoc* sp. R76DM (A) and dimeric (αβ) APC from *Lyngbya* sp. (B). The excitation wavelength for emission measurements was 589 nm.

Fig. 6. Far-UV CD spectrum of APC α-subunit in 20 mM phosphate buffer (pH 7.0) at 25 °C.

Fig. 7. Urea-induced denaturation study of single peptide APC α-subunit (A, C) and dimeric (αβ) APC (B, D). Changes in absorption spectra of APC α-subunit (A) and dimeric (αβ) APC (B) at pH 7.0 and 25°C, as urea increases from 0.0 to 6.0 M. Denaturation curves of APC α-subunit (C) and dimeric (αβ) APC (D) were constructed by following changes in $\Delta\varepsilon_{565}$ as a function of urea. Down arrow (↓) denotes absorption spectra of APCs with increasing [urea]

574 from 0.0 to 6.0 M. Circles and triangles showed the plot of $\Delta\varepsilon_{565}$ vs. urea during denaturation
575 and renaturation experiments, respectively.

576 **Fig. 8.** UV-visible spectra of single peptide PBP APC α-subunit after exposure to various
577 physico-chemical stressors such as temperature (A), pHs (B) and Oxidizing agent (C). The
578 down arrow (↓) denotes the absorption spectra of heat (4 ^{o}C: control, 20 ^{o}C, 40 ^{o}C, 60 ^{o}C and
579 80 ^{o}C.), pHs (7:control, 6, 4, 8, 2, 10 and 12) and H_2O_2 (control, 0.2, 0.4, 0.6, 0.8 and 1.0 %)
580 treated samples from top to bottom, respectively.

581 **Fig. 9.** SDS-PAGE of purified APC α-subunit at every 20 days up to 180 days (A) of storage
582 at 4 ^{o}C. SDS-PAGE of APC α-subunit isolated and purified from 10 to 60 days grown
583 cyanobacterium cultures. Z: zinc acetate and S: silver stained.

584

585

586 **Fig. 1.**

587

588

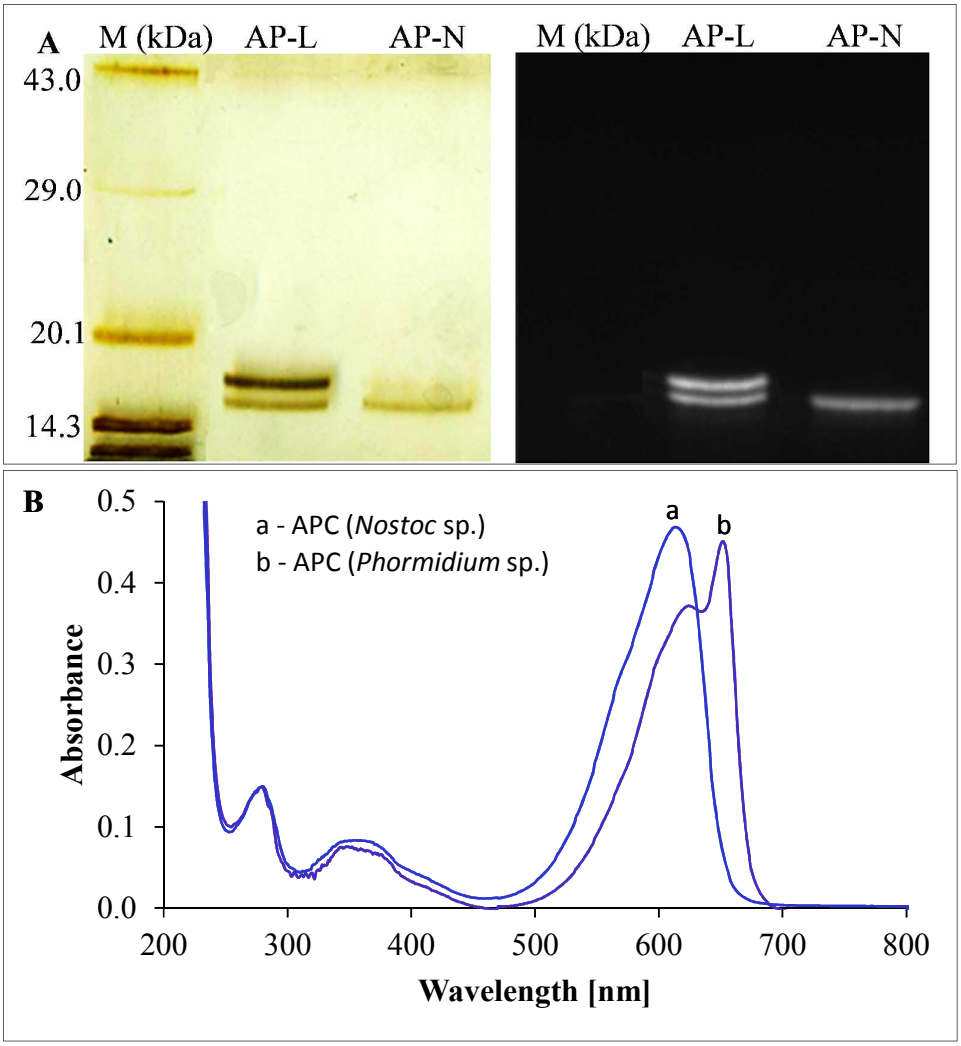

589

590

591 **Fig. 2.**

592

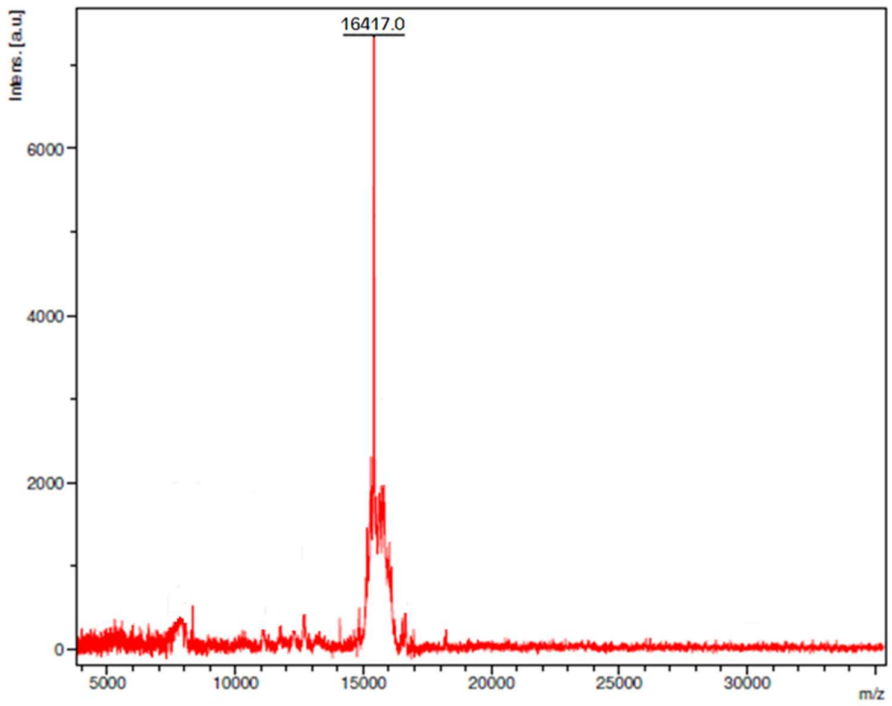

593

594

595

596

597

598

Fig. 3A

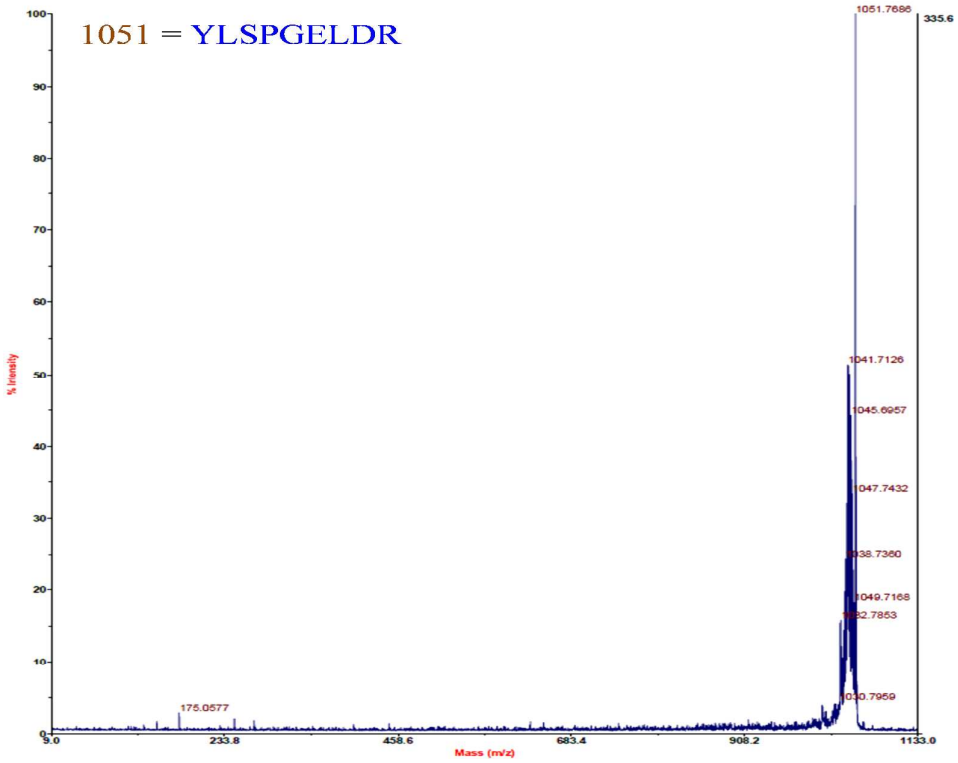

Fig. 3B

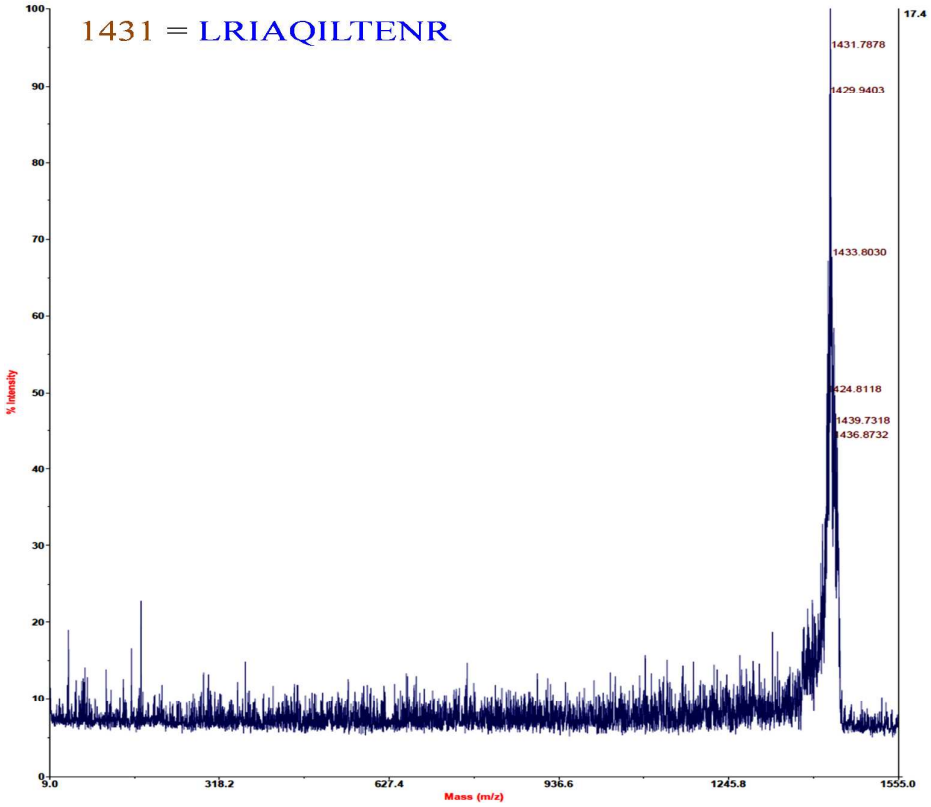

628 **Fig. 3C**

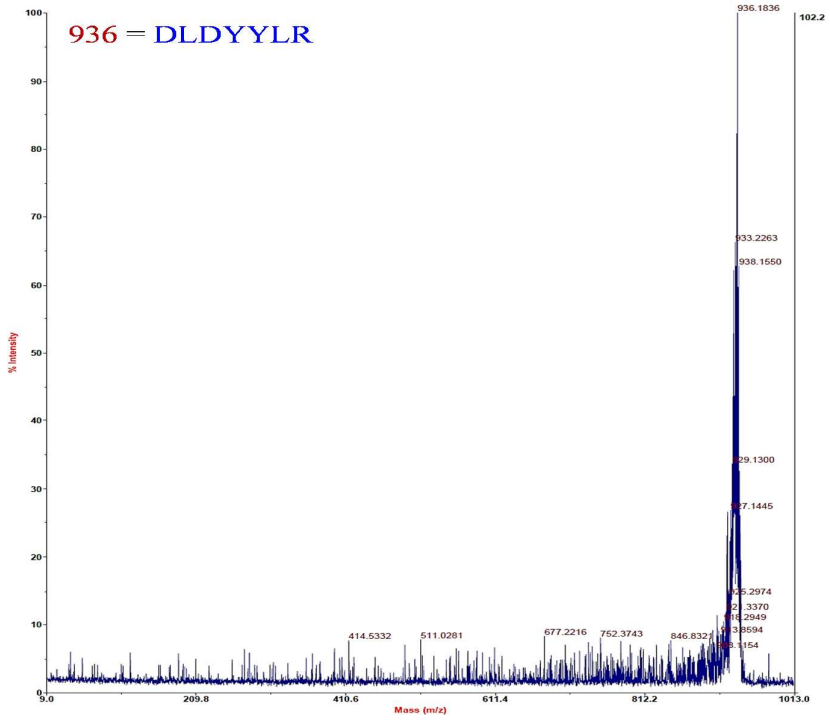

629

630

631

632

633

634

635

636

637

638

639

640

641

642

643 **Fig. 3D**

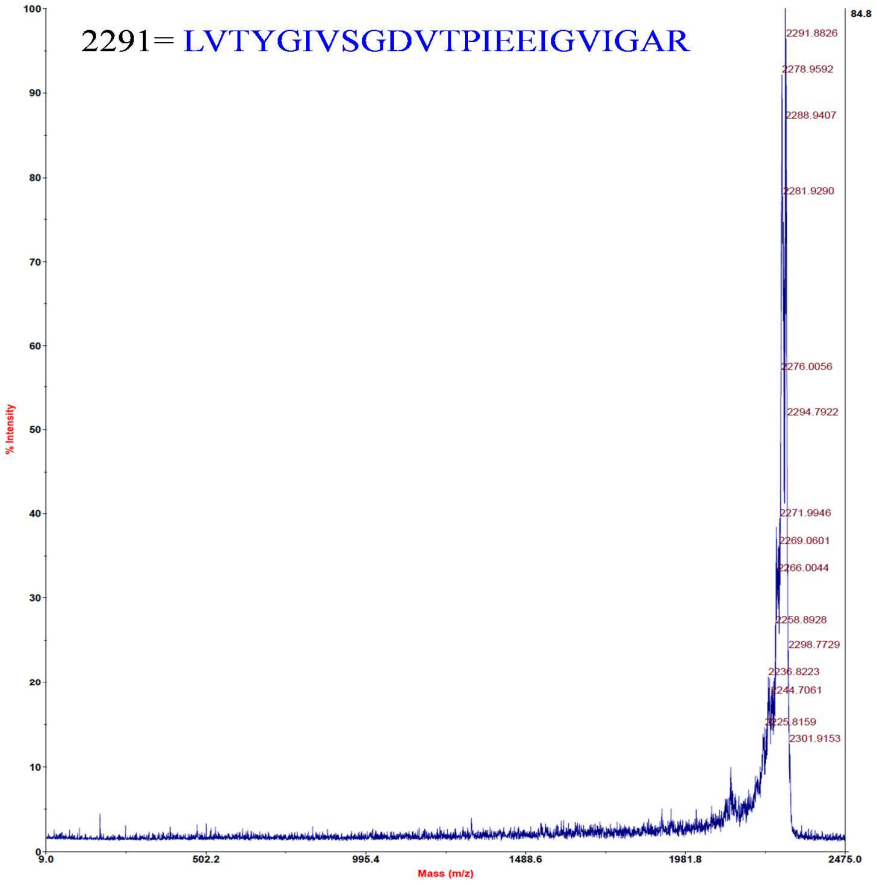

644

645

646

647

648

649

650

651

652

653

654

655

Figure 3E

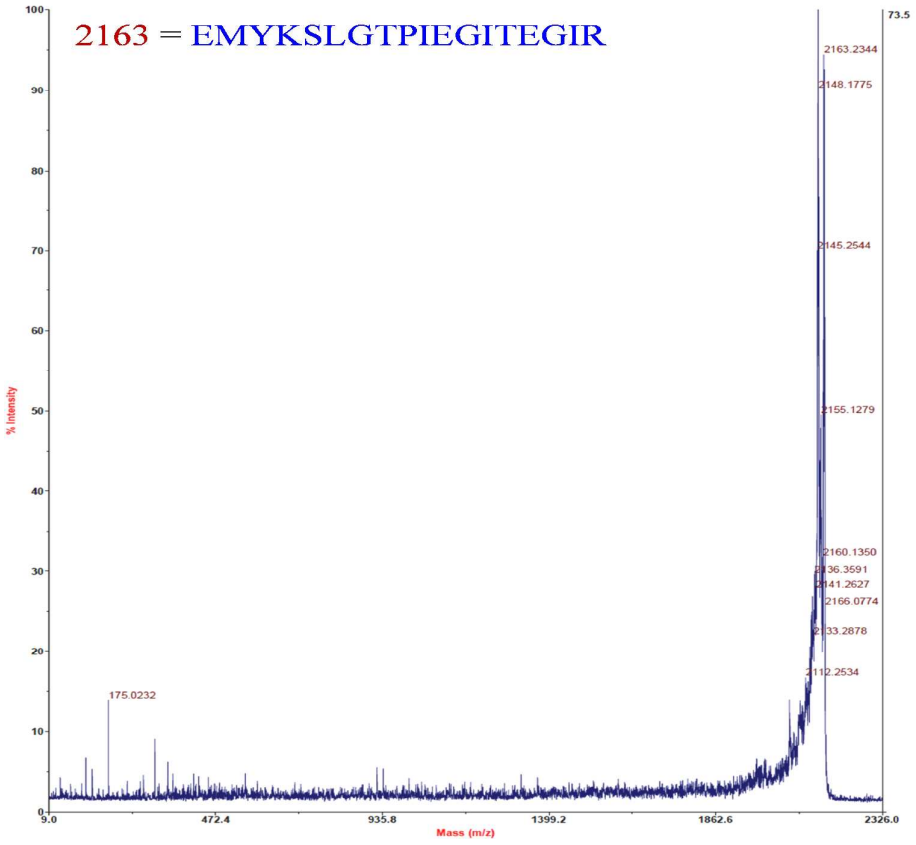

Fig. 3F

Aminoacid sequence of full Allophycocyanin alpha chain of *Microchaete diplosiphon* (Accession No. P16570)

MSIVTKSIVNADAEARYLSPGELDRIKSFVSGGERRLRIAQILTENRERLVKQAGEQVFQKRPDVVSPGGNAYGQ
ELTATCLRDLDYYLRLVTYGIVSGDVTPIEEIGVIGARLEMYKSLGTPIEGITEGIRALKSGASSLLSGEDAAEAGSY
FDYVVGALS

1051 1431 936 2291 2163

Fig. 4.

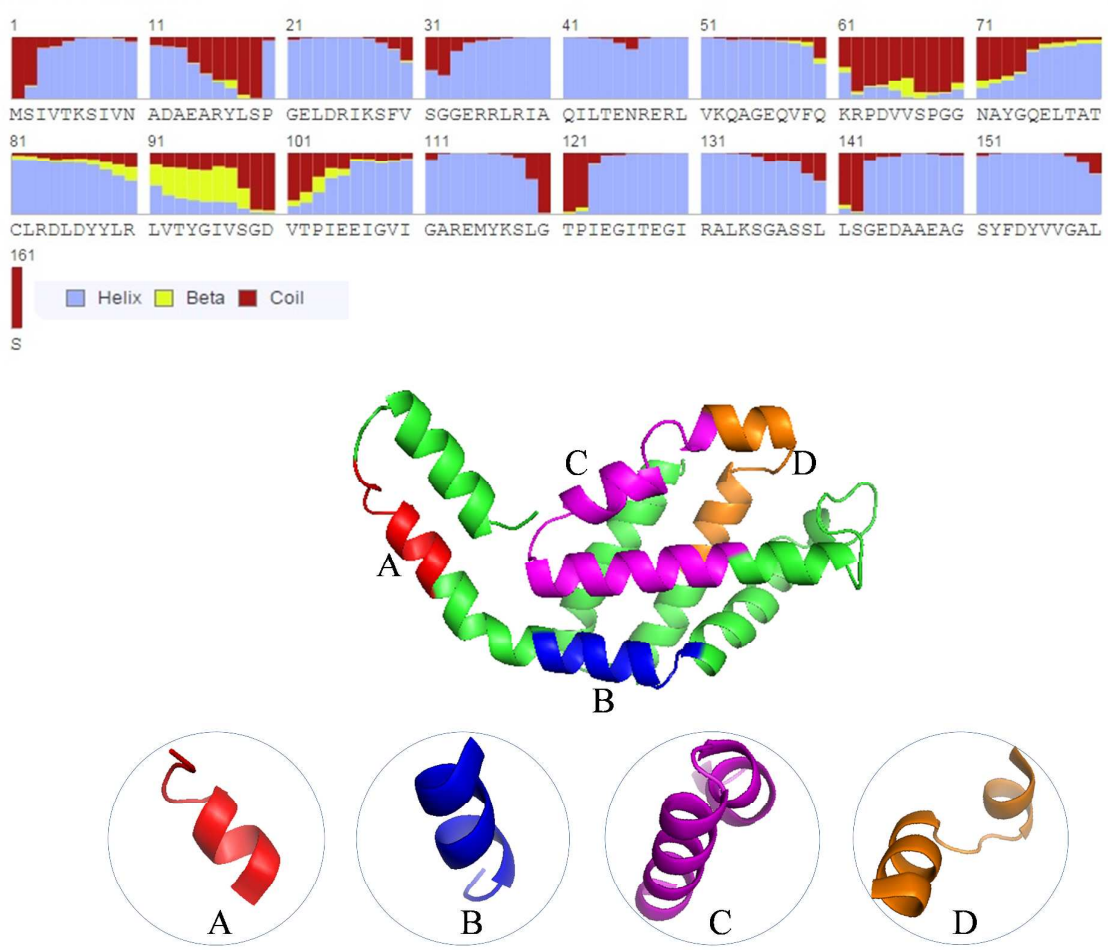

Fig. 5.

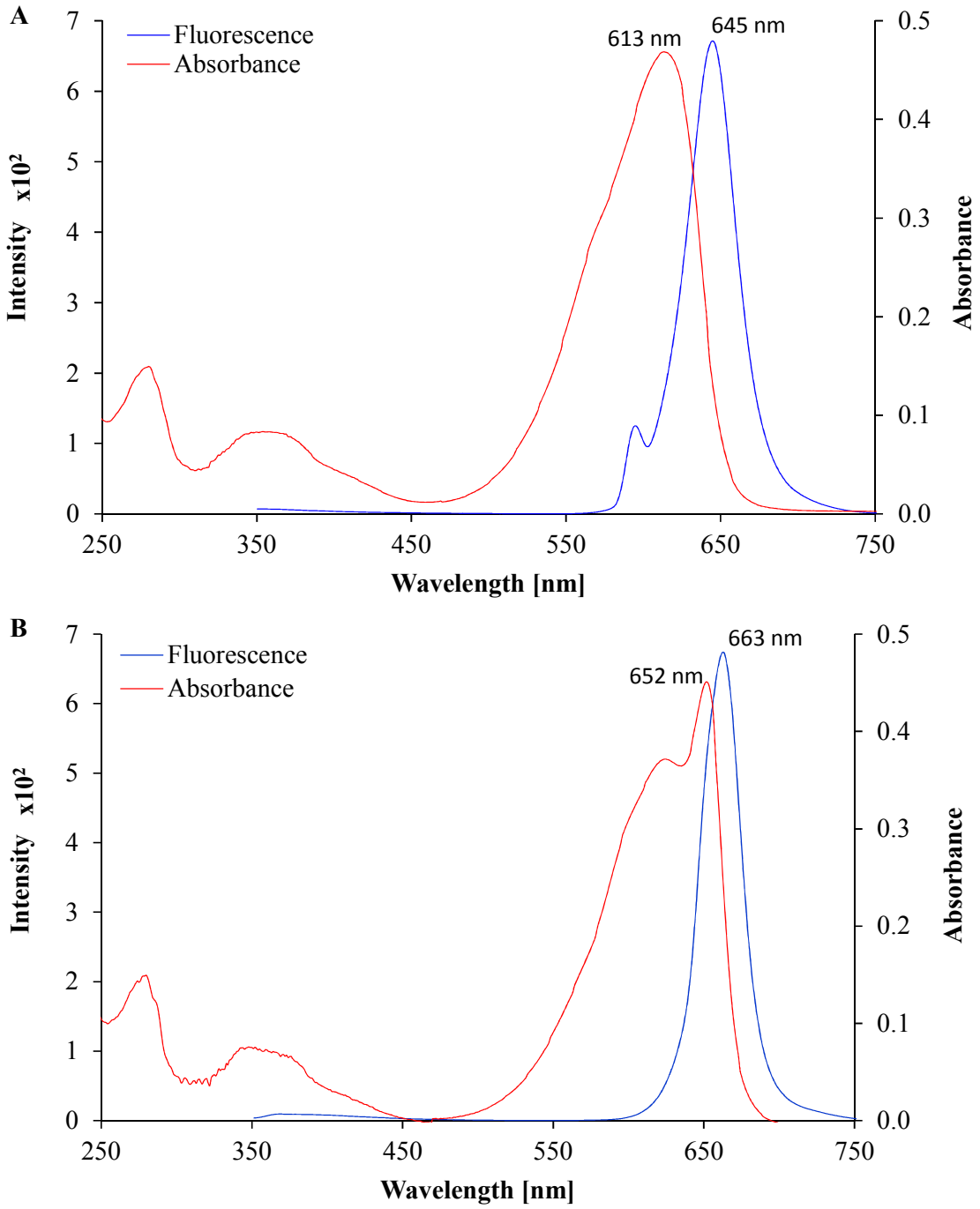

Fig. 6.

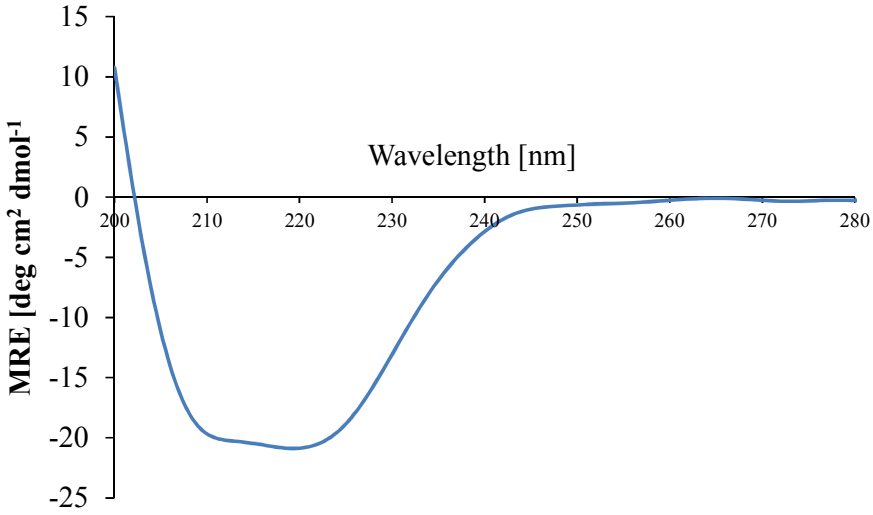

Fig. 7.

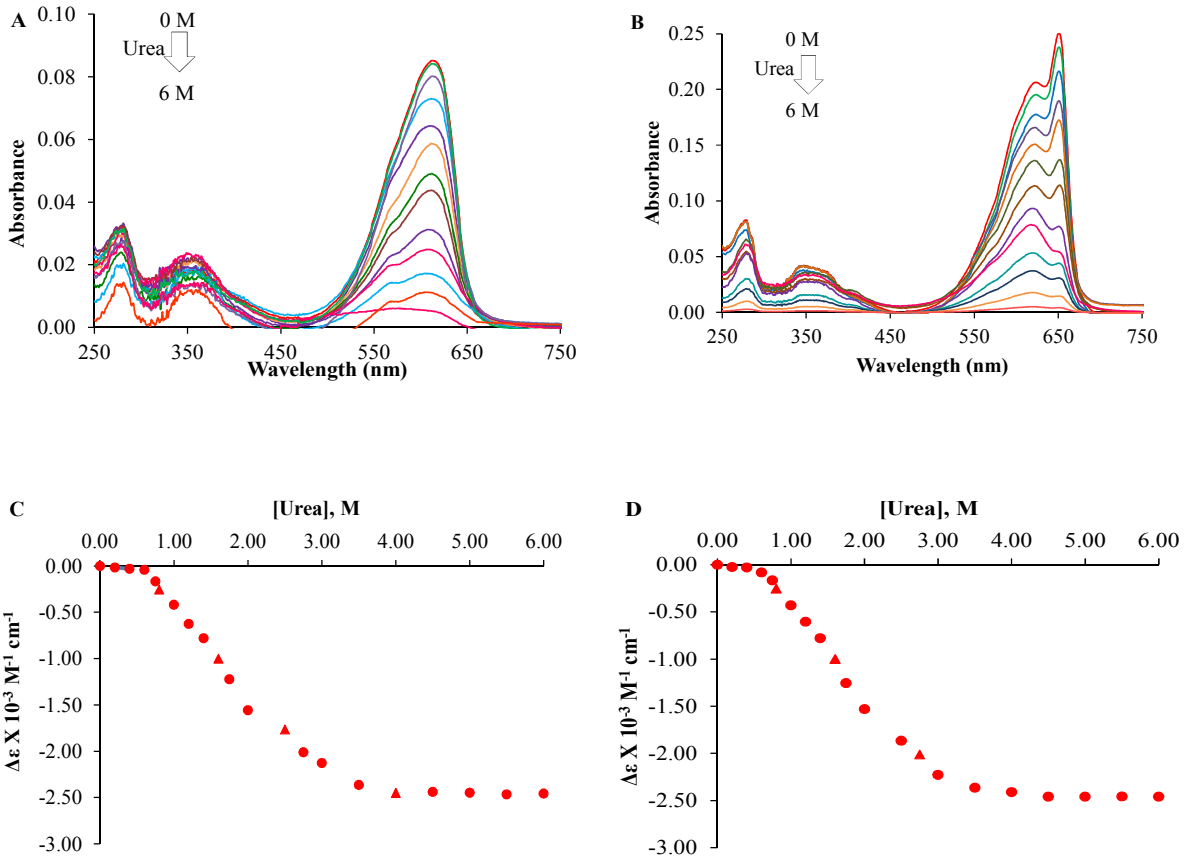

685

686

687

688

689

690

691

692

693 **Fig. 8.**

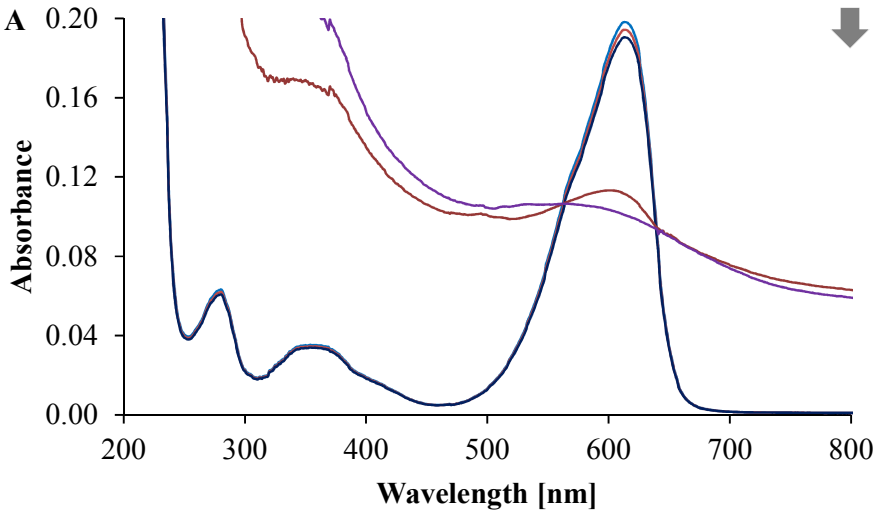

694

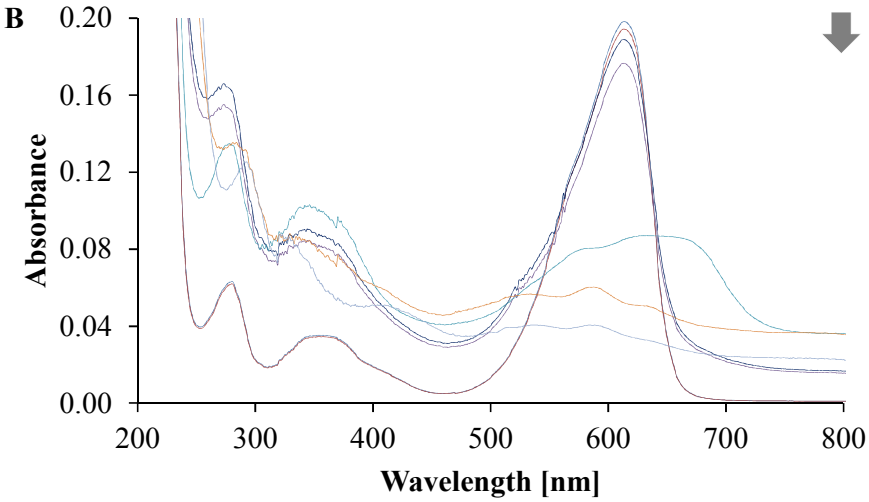

695

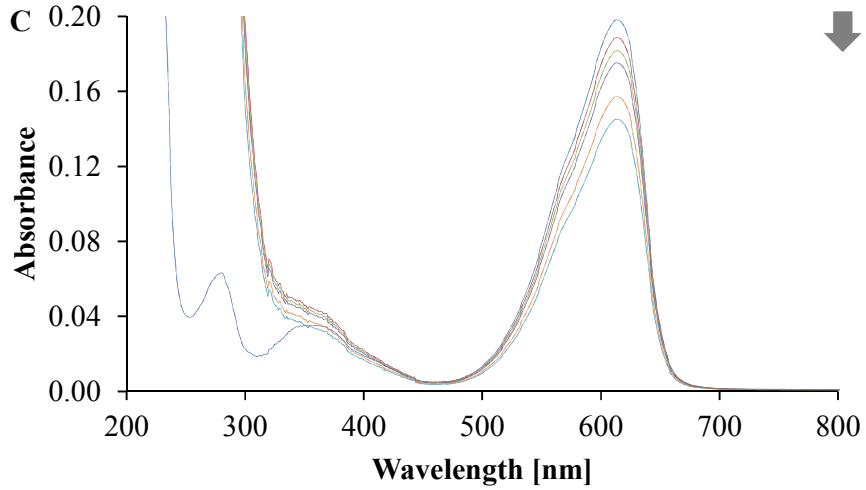

696

697

698 **Fig. 9.**

699

700

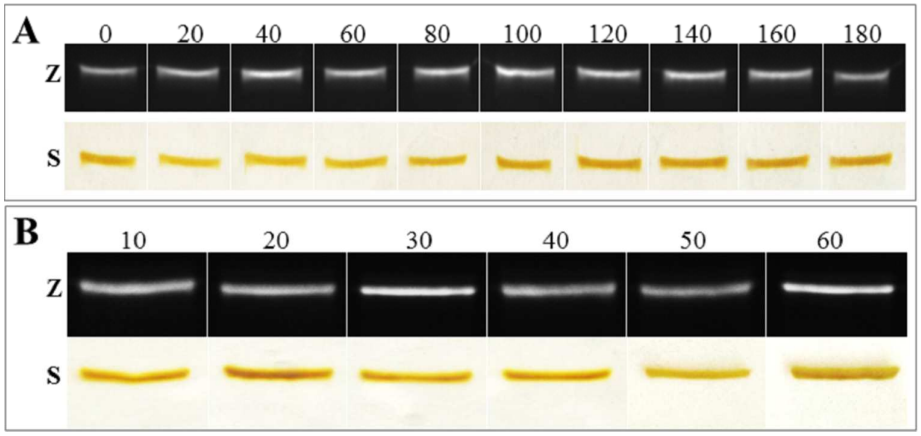

701

702

703

704